Volume 11 | Number 36 | 28 September 2015 | Pages 7069–7220

Soft Matter

www.softmatter.org

ISSN 1744-683X

ROYAL SOCIETY OF CHEMISTRY

PAPER
F. Weyer *et al.*
Compound droplet manipulations on fiber arrays

Soft Matter

PAPER

View Article Online
View Journal | View Issue

Cite this: *Soft Matter*, 2015, **11**, 7086

Received 11th February 2015,
Accepted 25th June 2015

DOI: 10.1039/c5sm00364d

www.rsc.org/softmatter

Compound droplet manipulations on fiber arrays†

F. Weyer,* M. Lismont, L. Dreesen and N. Vandewalle

Recent works demonstrated that fiber arrays may constitute new means of designing open digital microfluidic systems. Various processes, such as droplet motion, fragmentation, trapping, release, mixing and encapsulation, may be achieved on fiber arrays. However, handling a large number of tiny droplets resulting from the mixing of several liquid components is required for developing microreactors, smart sensors or microemulsifying drugs. Here, we show that the manipulation of tiny droplets onto fiber networks allows for creating compound droplets with a high complexity level. Moreover, this cost-effective and adjustable method may also be implemented with optical fibers in order to develop fluorescence-based biosensor.

I. Introduction

The study of static droplets on fibers has been extensively reported regarding their geometry, their wetting properties and their lifetime.[1–9] However, Gilet *et al.* demonstrated that droplets are also able to slide along fibers owing to the competition between gravity and capillarity.[10] In the case of crossed fibers, defining a fiber node, droplet motion studies have shown that, depending on the volume of the droplets, V, and the fiber diameters, they might either remain pinned at the node or continue their way by passing through the node, leaving behind tiny liquid amounts, as sketched in Fig. 1a. As shown in our previous work, this start–stop droplet motion along a fiber network may be used to separate an incoming droplet into several parts.[10] Additionally to the droplet fragmentation, fiber networks may also be used to cause the coalescence or the chemical reaction between droplets.[11] Another recent work proved that optical fibers network might be the starting point of optofluidic devices, allowing for probing the droplet content by spectrophotometry.[12] Despite droplet motions concern a wide range of applications, droplet evaporation constitutes the major drawback of these innovative techniques. A way to circumvent this limitation is based on the encapsulation of the water core droplet into an oil shell,[13] leading to the formation of a so-called *compound droplet*.

Currently, the development of compound droplets, made of an oil drop containing several inner aqueous droplets, are still essential considering scientific and technological applications such as multicompound capsules production, drugs transport, hazardous materials manipulation, microreactors creation or microbatteries fabrication. Although techniques are already implemented to create complex droplets,[14–24] we intend, by using fiber arrays, to develop an easy way to generate and handle such droplets as well as to explore the physics behind. Moreover, this original approach allows for better controlling both the droplet size and the number of components inside the oil droplet.

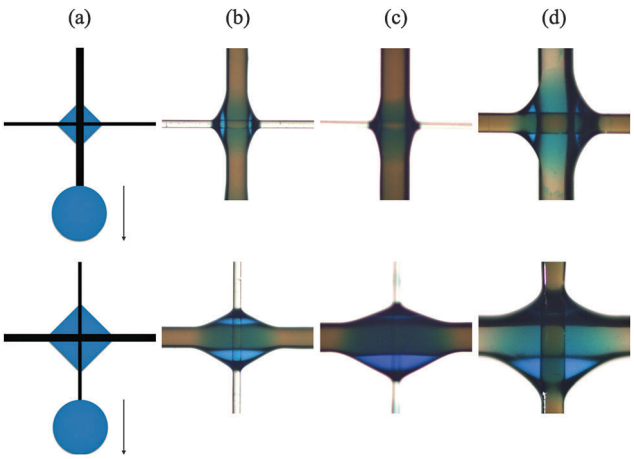

Fig. 1 Sketches and pictures of tiny residual droplets remaining at an asymmetric fiber crossings after the motion of a large droplet (8 μl) of colored water along the vertical nylon fiber. Four different cases are illustrated: (a) a schematic representation of a node made of two fibers with different diameters, (b) a water residue created at a crossing between a 80 μm diameter fiber and a 250 μm diameter fiber, (c) a water residue created at a crossing between a 80 μm diameter fiber and a 350 μm diameter fiber, and (d) a water residue created at a crossing between a 250 μm diameter fiber and a 450 μm diameter fiber. Obviously, the volume of the residue depends on the fiber diameters. For each type of node, two configurations are possible: (top) the thicker fiber is vertical or (bottom) the thicker fiber is horizontal. The residues are quite different for these two situations: When the thick fiber is horizontal, the remaining droplet is seen to be much larger.

GRASP, Physics Department, University of Liège, Allée du 6 Août, 19, B-4000 Liège, Belgium. E-mail: f.weyer@ulg.ac.be

† Electronic supplementary information (ESI) available. See DOI: 10.1039/c5sm00364d

Our results are decomposed in three major successive steps. First, we show how to create the inner droplets through the droplet fragmentation at the network nodes. Second, we explain how tiny droplets can be released from the nodes using encapsulation by oil. Both colored and fluorescent inner droplets were considered. Finally, we combine fragmentation and release processes to create complex compound droplets, also called multicompound droplets.

II. Experimental

In order to achieve our tasks, we used a rigid frame in which nylon fibers or optical fibers are horizontally and vertically stretched to create a fiber network with a set of crossings. Since the fiber diameter drives droplet motions, we investigate networks of fibers with diameters ranging from 80 μm to 450 μm. Prior to experiments, nylon fibers were cleaned with acetone and distilled water before drying. Before their use, the multimode optical fibers with a diameter of 400 μm are prepared as follow. From their distal end, 5 cm of the external jacket was removed with a fiber buffer stripping tool. The uncovered regions of fibers were cleaned with acetone and were rinsed with distilled water.

Droplets are formed using a mixture of SDS in water (0.01 M) in which dye is added for getting stronger contrast. This mixture has a density $\rho_l = 1000$ kg m^{-3} and a viscosity $\nu_l = 1$ cSt. When optical fibers are used, fluorophores are dissolved inside the water solution instead of dye. Fluorescein and rhodamine were considered. The SDS molecules reduce the water surface tension and thus the contact angle of the droplet and so allow for generating barrel shaped droplet, which consists in a rotational symmetric pearl-like structure. Water droplets are left on the network and slide along the fibers. The water droplets pinned at the nodes are encapsulated by oil. We used a silicone oil (Dow Corning) with a density $\rho_o = 950$ kg m^{-3}. Oil viscosity can affect the multicompound droplet lifetime so we investigate the encapsulation of water droplets with several viscosities ranging from $\nu_o = 10$ cSt to $\nu_o = 1000$ cSt. Oil and liquid mixtures are characterized by low surface tensions and are therefore wetting the fibers. The surface tensions have been determined using the pendant drop method using a CAM 200 goniometer from KSV Instruments Ltd. The air-colored liquid surface tension is found to be $\gamma_l = 25.7 \pm 0.1$ mN m^{-1}. The air–oil tension is $\gamma_o = 18.5 \pm 0.3$ mN m^{-1}. The oil-colored liquid tension is much smaller: $\gamma_{ol} = 5.5 \pm 0.1$ mN m^{-1}.

III. Results and discussion

Droplet fragmentation

In this section, we focus on the interaction between a water droplet and a node, which leads to the formation of a residue, a tiny droplet that will be encapsulated in an oil drop (see next section).

When a single liquid droplet glides on a vertical fiber of diameter b, the droplet motion can be stopped by a horizontal fiber of diameter a. If capillarity overcomes gravity, the droplet sticks at the node. This occurs for a droplet volume smaller than a critical volume, V_{stop}, given by

$$V_{stop} = \frac{\xi \gamma_l a}{\rho_l g} \quad (1)$$

where ρ_l is the liquid density, g is the gravity acceleration and $\xi \approx 1.124\pi$ is a shape factor which mainly depends on the node geometry as shown by Gilet *et al.*[11] This V_{stop} corresponds to a critical Bond number, $Bo^* = \rho_l V_{stop} g/4\pi\gamma_l a = 1.12$ which seems to be constant for viscosities higher than 20 cSt.[11] For example, typical aqueous solutions on 200 μm nylon fibers imply $V_{stop} \approx 5$ μl. The fiber diameter a can be selected in order to trap droplets at selected sites on the array. If the incoming volume is larger then V_{stop} (if $Bo > Bo^*$), the droplet slows down at the crossing, wets both fibers and detaches from the node leaving a tiny residual volume.

Pictures of Fig. 1 show the residual droplets created after the crossing of a 8 μl water droplet at different fiber nodes. In this figure, (a) is a sketch of the crossings and (b), (c), and (d) are three different asymmetric nodes, *i.e.* made of two fibers with different diameters ($a \neq b$). For each crossing, top row presents the case for which the thicker fiber is vertical and the thinner one is horizontal while the bottom row presents the same systems rotated by 90°.

The remaining volume, V_r, is much smaller than V_{stop} and is expected to be strongly dependent on the geometrical parameters of the node such as the fiber diameters or the fiber crossing angle, but also on physical characteristics of the liquid. The equilibrium shape is non-trivial but looks like a diamond. Indeed, each residue surrounds both horizontal and vertical fibers and wets these fibers with a non-zero contact angle. The smallest residues are symmetrical about both fibers. However, for the largest volumes, the residual droplets are slightly off-center due to gravity. The residue shape is similar for all wetting liquids. However, for non-wetting fluids, the incoming droplet is asymmetric and therefore the process is different. Fig. 1 shows that, by increasing the fiber diameters, the residual volume is increased. However, it has to be noticed that, for nodes with two different fibers, not only the diameter matters but also the orientation of these fibers. Indeed, the situation is completely different when the thick fiber is either vertical ($a < b$) or horizontal ($a > b$). It appears that a larger residual droplet remains at the node when the thick fiber is horizontal. The typical volume of such droplets is ranging from 1 μl on thick fibers down to 0.01 μl for thin fibers. The latter volume is close to the one produced in closed microfluidic systems composed of channels.[16–23,25] The manipulation of such tiny droplets on fibers opens therefore an alternative way to design microfluidic systems.

The volume V_r of the residual droplets has been measured for a wide range of nodes: not only different diameters but also different combinations of thin and thick fibers have been considered. The data are obtained by estimating the volume remaining at each node type from image analysis, as described in ESI.† Fig. 2a and b show the residual volume (V_r) evolution as a function of the horizontal diameter a in the case of a vertical fiber with a diameter b of 80 μm and 300 μm, respectively. These plots highlight the strong dependence between the residual volume and the diameter, a, of the horizontal fiber.

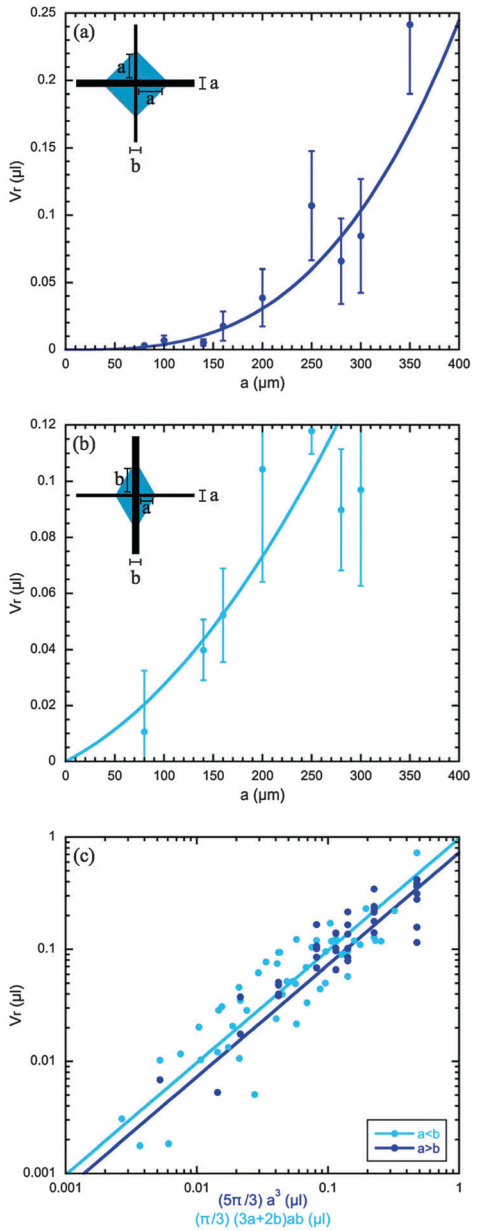

Fig. 2 (a) and (b) Plots of the residual volume, V_r, at a fiber crossing, as estimated by image analysis, as a function of the horizontal fiber diameter a. Data are shown for a fixed vertical diameter: (a) b = 80 µm corresponding to $b < a$ and (b) b = 300 µm corresponding to $b \geq a$. The curves correspond to the model proposed by eqn (2). (c) The residual volume as a function of the suggested model shown for a large range of fiber diameters. Dark blue dots correspond to data with $b < a$ and light blue dots correspond to data with $b \geq a$. The straight lines correspond to the linear fits of the data. The shape factors are found to be $\zeta = 0.73 \pm 0.05$ for $b < a$ and $\zeta' = 0.97 \pm 0.06$ for $b \geq a$. The plot highlights the linear dependence between the volume and the model. Moreover, the log–log plot emphasizes the wide range of volumes, *i.e.* over three decades, remaining on the fiber nodes.

As a increases, V_r becomes larger. The results are robust and seem independent of the volume of the incoming water droplet.

We consider that the droplet fragmentation is entirely determined by the deformation of the droplet at the fiber crossing after being strongly slowed down, meaning that the capillary effects dominate the viscous ones and so that the fragmentation in independent of the incoming droplet speed. In order to confirm this assertion, we studied the droplet speed by analyzing movies of the incoming droplet motion. The droplet reaches its limit speed after 10 ms and a distance of 1 mm.[11] The typical droplet speed is found to be close to 0.1 m s^{-1} at the node. The capillary number Ca, defined as $Ca = (\nu_l \rho_l v)/\gamma_l$ and corresponding to the ratio between the viscous forces and the capillary forces, is calculated and is found to be equal to 0.004. As Ca is much smaller than 1, viscous effects can be neglected. Therefore, we propose a model in which the shape of the residues only depends on capillary effects. Since the residual droplet has a diamond shape, we assume in a first approximation that it is made of four right triangles with a basis and a height corresponding to characteristic lengths that we need to determine. By looking at the pictures and the data, it appears that the residual volume mainly depends on the horizontal fiber diameter. When the incoming droplets crosses the node, it experiences a deformation with a characteristic length a as the wetting is directly related to the fiber diameter. The size of the horizontal fiber determines the size of the residual droplet. Therefore, we assume that the triangle has a basis and a height a. This assumption is correct as long as b is smaller than a. However, when b is larger than a, the vertical fiber influences the residual volume. The residual droplet is modified and is spread along the vertical fiber. In this case, we assume that the triangle height is no longer a but rather b. Thus, we have to distinguish two regimes: $b < a$ and $b \geq a$. In the first one, only the horizontal diameter matters whereas, in the second one, both horizontal and vertical fibers influence the residual volume. For each case, the rotation of the corresponding triangle around the horizontal fiber using the Pappus–Guldinus theorem gives the approximate residual volume

$$V_r = \begin{cases} \zeta \frac{5\pi}{3} a^3, & \text{if } b < a, \\ \zeta' \frac{\pi}{3}(3a + 2b)ab, & \text{if } b \geq a. \end{cases} \quad (2)$$

where ζ and ζ' are shape factors. In order to validate our model, we plot, in Fig. 2c, the measured residual volume as a function of $(5\pi/3)a^3$ and $(\pi/3)(3a + 2b)ab$. The data are plotted in a log–log scale since the residual volumes are distributed over three decades. We found that $\zeta = 0.73 \pm 0.05$ in the first case and $\zeta' = 0.97 \pm 0.06$ in the second one. The data show that V_r depends linearly on a^3 when $b < a$ and on $(3a + 2b)ab$ when $b \geq a$. The scaling proposed in our model is consistent with our data. In Fig. 2a and b, the model curves are represented by the solid lines for b = 80 µm and b = 300 µm corresponding to $b < a$ and $b \geq a$, respectively. The agreement between the model and the data is satisfactory on both plots. Only numerical simulations could improve the measurement of the residual volumes. Finally, an asymmetry between horizontal and vertical fibers is visible in the model. Indeed, for asymmetric nodes, the residual volume depends on the fiber orientation. When rotating the node with a 90° angle, the system switches from the case $b < a$ to the one $b \geq a$ or *vice versa* and therefore, the residual volume

is different. According to eqn (2), for a given node, the residual volume is larger when the thickest fiber is horizontal than when it is vertical. Therefore, our model is consistent with our observations: the volumes are different when swapping a and b, *i.e.* when the system is rotated by 90° as it is shown in Fig. 1.

Releasing microdroplets

After having studied the fragmentation of a large droplet and having characterized the residual volume, the detachment and the collection of the residue is investigated in order to create a compound droplet. The fragmentation process of a large droplet into several tiny volumes can be implemented on a vertical array of fibers. The method allows for controlling both position and volume of each tiny droplet. However, the release of a specific residue could be seen as a non-trivial task. Indeed, once formed, the residual volume V_r is trapped at the node because it is much smaller than V_{stop} and therefore the capillary forces hold the residue at the crossing whether the fibers are rotated or agitated. We investigate the droplet release by launching an oil droplet. This oil drop will encapsulate the residue and will release it in some specific conditions.

Once the water residue is created with a volume V_r, an oil droplet is launched on the vertical fiber and meets the residual water droplet at the node. The competition of air/oil/water surface tensions leads to the encapsulation of the aqueous droplet by oil. This process takes place[25,26] if

$$\gamma_l > \gamma_o + \gamma_{ol} \quad (3)$$

which is verified in our case (see Experimental for the values of the surface tensions). At this point, a compound droplet is formed at the node. It is made of a water droplet centered on the crossing and surrounded by the oil droplet. Then, the instantaneously formed compound droplet detaches from the node when its global volume is larger than V_{stop} and leaves a residue given by V_r following the same process as described in the previous section. As the water volume trapped at the node before the oil droplet arrival was already V_r, the aqueous droplet remains trapped at the node and the oil droplet just leaves a thin oil film and does not release any water. Therefore, after the oil droplet crossing, the water residue is still trapped at the node and the oil droplet continues its descent without containing any aqueous droplet. This process is sketched in Fig. 3a and b. The top row presents the aqueous residue formation at the same node except that the fibers in (b) are rotated by 90° with respect to (a), leading to a slightly larger volume V_r. However, in both cases, when an oil droplet glides on the vertical fiber, it just wraps the residue, leaves a thin oil layer around the water residue trapped at the node and continues its way, along the vertical fiber, without collecting any water (middle row). Thus, at the end, the oil droplet, stopped thanks to a much larger horizontal fiber, does not contain water (bottom row). In order to release water residues, increasing the volume at the node by adding oil is not sufficient. Taking advantage of the asymmetry of the residues when a and b are switched is a solution. Indeed, on Fig. 3c, an aqueous residue, with a volume V_r is created while the thicker fiber is horizontal (top row). The system is

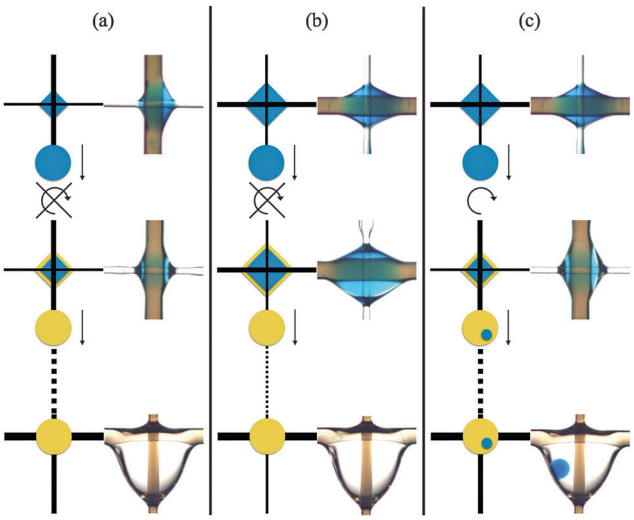

Fig. 3 Sketch of the creation and the collection of the residues. For the three cases, first (top row), a large water droplet (8 μl) crosses a node and leaves a residue. Second, an oil drop (4 μl) glides along the fiber and crosses the node (middle row). Finally (bottom row) the oil droplet continues its way and is stopped by a larger horizontal fiber. In the first two cases, the thicker fiber remains vertical (a) or horizontal (b) during the whole process. Therefore, once the residue is created at the node, it remains trapped and no water is released from the node. Whereas, in case (c), the thicker fiber is horizontal during the creation of the water residue and then, after the rotation of the system by 90°, it becomes vertical and, the residual volume is, now, larger than expected and therefore the oil droplet releases the exceeding volume of water.

then rotated by 90°, so that the thicker fiber is vertical and the thinner one is horizontal. At this stage, the volume of the residue is larger than expected with eqn (2) because it was created while the thick fiber was horizontal. However, this volume still smaller than V_{stop}, thus it remains at the node. Therefore, when the oil droplet arrives at the node, the excess volume is dragged by the oil droplet and is encapsulated inside the moving droplet. A tiny residue is so trapped at the node with the volume expected for this fiber configuration (middle row). At the end of the fiber array, the oil droplet is stopped by a crossing of two large fibers. Compared to cases (a) and (b), the oil droplets contains a tiny aqueous droplet. One would notice that the collection process only occurs if the residue, created before the rotation, is larger than the residue left after the oil droplet crossing. Therefore, according to the previous section, the water residue should be created when $a > b$. Optical effects, due to the oil shell surrounding the inner droplets, prevent the measurement of precise water volume by image analysis. However, the inner water droplet should have a typical volume of 0.1 μl.

The collection process is a phenomenon driven by capillary effects. Indeed, as defined in the previous section, the capillary number has been calculated for the oil droplet motion. Depending on the oil viscosity (ranging from 10 cSt to 1000 cSt), the Ca varies from 0.006 and 0.6. As the capillary number is always smaller than 1, we can assume that capillarity overcomes viscosity. Therefore, the collection process should be independent from the oil viscosity. In order to validate this assumption, we tried to

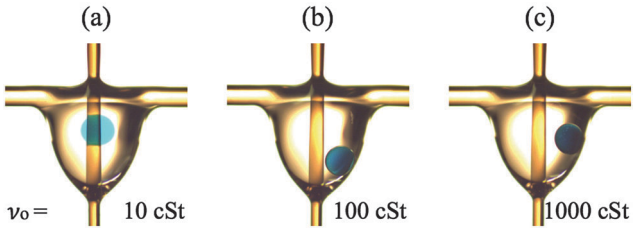

Fig. 4 Pictures of oil droplets containing a water component. All droplets have been created with the same device. However, the oil viscosity is different: (a) 10 cSt, (b) 100 cSt and (c) 1000 cSt. These pictures prove that the collection process occurs regardless of the oil viscosity.

collect water residues with oil droplets of different viscosities, ranging from 10 cSt to 1000 cSt, by using the same fiber array. Fig. 4 shows the oil droplets, at the final node. Each droplet contains a water component regardless of its viscosity. Moreover, the inner water droplets appear to have the same volume.

These results show that the encapsulation allows for releasing a residue trapped at a node. When the oil droplet reaches the node, the excess water volume detaches so that the oil droplet contains a water component. This process is similar to dripping such that the main relevant parameter is the geometry of the node. But more importantly, the rotation of 90° provides an exchange of thick and thin fibers such that the release is triggered.

Complex compound droplets

The last step in creating multicompound droplets is to encapsulate more than one inner droplet. By repeating the release of tiny droplets, we can increase the number of inner droplets and therefore create a highly sophisticated droplet. Here, we prove that using fibers is also a suitable way to generate droplets with multiple inner components. The principle for creating multicomponent droplets is sketched on Fig. 5a. Here, four vertical fibers are used to create four residues on a single horizontal fiber. As the droplets are wetting the fibers and are large enough, they cross the node and they each leave a residue. The remaining tiny droplets are on a common fiber which is then placed vertically, by rotating the whole fiber array by 90°. A silicon oil droplet is then released from top to bottom. This droplet collects a proportion of every droplet and form a compound system. A larger fiber at the bottom of the array stop the motion of the silicon oil droplet, allowing for analysis or further delivery. Without this terminal horizontal fiber, the compound droplet can detach from the fiber array and be transferred to another device. A single row of fiber nodes is therefore needed for creating a compound droplet. Since increasing the oil viscosity increases the lifetime of the inner droplets but also the duration of the whole process, we chose to use a 100 cSt oil.

The first picture in Fig. 5b illustrates the generation of a compound droplet containing four different inner components. The four different colors inside the droplet prove that the oil drop has collected a part of every water droplet. The number of inner components can be increased as shown in the second and the third pictures of Fig. 5b with five and six inner droplets.

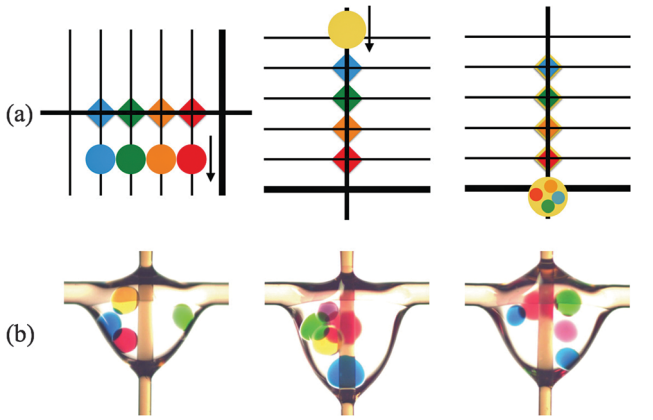

Fig. 5 (a) Sketch of the basic principle to create compound droplets. We use an array of fibers of different diameters. First, four water droplets of different colors slide along the vertical fibers, cross the nodes and leave a residue. Second, the system is rotated and an oil drop glides along the new vertical fiber and collects a part of each water residue. In the end, a compound droplet is obtained. (b) Picture of multicompound droplets obtained by using the device sketched in (a). By changing the number of fibers, the number of inner droplets can be increased.

These pictures prove that our technique is efficient at generating multicompound droplets. A 2D/3D array could provide a promising way to multiplex or handle a much larger set of droplets.

IV. Conclusion

The fabrication of a complex droplet by encapsulating tiny drops has an enormous potential for scientific and technological applications in pharmaceutical drug delivery, biosensors, soft materials, microreactors, food science, cosmetics, *etc.* These highly sophisticated objects are, currently, widely studied.[14–24] Microfluidic devices have been invented for producing some elaborated fluidic objects, also called multicompound droplets. However, we proved herein that fiber arrays provides a basis for a new type of microfluidic devices able to produce highly sophisticated droplets, as illustrated in Fig. 5b. We first showed how a droplet interacts with a crossing leading to the formation of residues. Second, we proposed a technique for collecting those water droplets inside an oil drop. And finally, we obtained compound droplets by using this process. The device is very effective because the number and the volume of the inner drops can be controlled by selecting the fiber diameters. Placing different pure components on different fibers avoids the contact between them and allows them to remain separate inside the oil drop once they are collected. Moreover, the coalescence of the inner droplets can be triggered by using a specific paraffin (Suppocire AIM oil[16]) instead of oil. The only limitation of this process is the evaporation of the water components before their collection by the oil droplet. This will be addressed in our future works. However, this multicomponent droplet production offers a number of possibilities. Indeed, arrays can be designed for generating, on a single device, all possible combinations of liquid mixtures starting from few drops (see ESI†). Once created, several complex droplets can also be manipulated on the same array. As shown in Fig. 6a, reactions can also take place

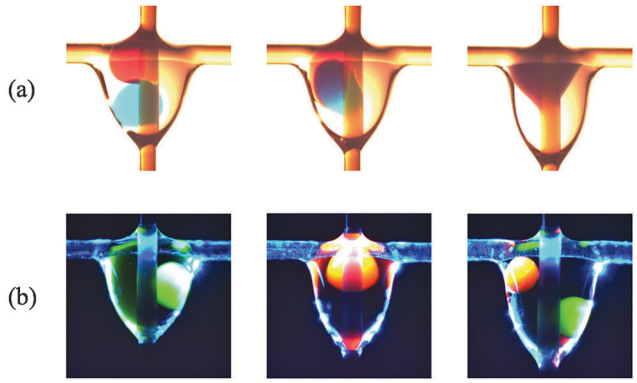

Fig. 6 Pictures of several applications of compound droplets. (a) The evolution of the inner components over time. Reagents can be placed inside the components and interact after the fusion of the droplets. This reaction is represented by the change in colors after the coalescence. (b) By replacing the horizontal fiber by an optical one, fluorescence of inner droplets can be excited. Fluorescein and rhodamine are excited by a blue laser and produce a green and orange fluorescence, respectively.

inside a compound droplet. Reagents, placed in the inner components, interact together after the fusion of the inner droplets. This type of reaction is represented by the mixture of the colors after the coalescence of the drops. Moreover, when encapsulated drops are engineered for being microreactors or smart sensors, the fibers themselves could be used to excite fluorescence or to measure an optical signal from the inner drops. Fig. 6b shows that it is possible to excite and detect the fluorescence of the components by using optical fibers coupled with a laser. A 488 nm laser beam is guided into a multimode fiber through a fiber coupler. The incident light propagates along the fiber and interacts with the fluorophores dissolved inside the inner droplets. The fluorescence light is then collected by the other optical fiber and is conveyed to a CCD spectrometer. This technique has already been validated in our lab.[12] However, in this work, it is applied to the water droplets inside the oil shell. Fibers provide therefore an original way to create and manipulate compound droplets. This effective and adaptable method makes possible the applications requiring highly sophisticated droplets.

Authors contributions statement

FW and ML collected and analyzed experimental data. Physical interpretations were provided by all authors. This manuscript was written by FW and NV.

Competing interests

The authors declare that they have no competing financial interests.

Acknowledgements

We sincerely thank Guillaume Lagubeau for helpful discussions. FW thanks FRS-FNRS for financial support. This work is financially supported by FNRS (Grant FRFC 2.4504.12) and by the University of Liège (Grant FSRC-14/03).

References

1 G. McHale, M. I. Newton and B. J. Carroll, *Oil Gas Sci. Technol.*, 2001, **56**, 47.
2 G. McHale and M. I. Newton, *Colloids Surf., A*, 2002, **206**, 79.
3 P. G. de Gennes, F. Brochard-Wyart and D. Quéré, *Capillarity and wetting phenomena: drops, bubbles, pearls, waves*, Springer Science & Business Media, 2004.
4 E. Lorenceau, C. Clanet and D. Quéré, *J. Colloid Interface Sci.*, 2004, **279**, 192.
5 A. Sauret, A. D. Bick, C. Duprat and H. A. Stone, *Europhys. Lett.*, 2014, **105**, 56006.
6 F. Mugele, M. Duits and D. van den Ende, *Adv. Colloid Interface Sci.*, 2010, **161**, 115.
7 H. B. Eral, J. de Ruiter, R. de Ruiter, J. M. Oh and C. Semprebon, *et al.*, *Soft Matter*, 2011, **7**, 5138.
8 R. Dufour, A. Dibao-Dina, M. Harnois, X. Tao and C. Dufour, *et al.*, *Soft Matter*, 2013, **9**, 492.
9 C. Duprat, A. D. Bick, P. B. Warren and H. A. Stone, *Langmuir*, 2013, **29**, 7857.
10 T. Gilet, D. Terwagne and N. Vandewalle, *Eur. Phys. J. E: Soft Matter Biol. Phys.*, 2010, **31**, 253.
11 T. Gilet, D. Terwagne and N. Vandewalle, *Appl. Phys. Lett.*, 2009, **95**, 014106.
12 M. Lismont, N. Vandewalle, B. Joris and L. Dreesen, *Appl. Phys. Lett.*, 2014, **105**, 133701.
13 F. Weyer, L. Dreesen and N. Vandewalle, arXiv:1505.0526, unpublished work.
14 C. Planchette, E. Lorenceau and G. Brenn, *Colloids Surf., A*, 2010, **365**, 89.
15 C. Planchette, E. Lorenceau and G. Brenn, *J. Fluid Mech.*, 2012, **702**, 5.
16 L. L. A. Adams, T. E. Kodger, S.-H. Kim, H. C. Shum and T. Franke, *et al.*, *Soft Matter*, 2012, **8**, 10719.
17 P. B. Umbanhowar, V. Prasad and D. A. Weitz, *Langmuir*, 2000, **16**, 347.
18 A. S. Utada, E. Lorenceau, D. R. Link, P. D. Kaplan and H. A. Stone, *et al.*, *Science*, 2005, **308**, 537.
19 L.-Y. Chu, A. S. Utada, R. K. Shah, J.-W. Kim and D. A. Weitz, *Angew. Chem.*, 2007, **46**, 8970.
20 A. R. Abate, A. Rotem, J. Thiele and D. A. Weitz, *Phys. Rev. E: Stat., Nonlinear, Soft Matter Phys.*, 2011, **84**, 031502.
21 S. Okushima, T. Nisisako, T. Torii and T. Higuchi, *Langmuir*, 2004, **20**, 9905.
22 T. Nisisako, S. Okushima and T. Torii, *Soft Matter*, 2005, **1**, 23.
23 N.-N. Deng, C.-L. Mou, W. Wang, W.-J. Ju, R. Xie and L.-Y. Chu, *Microfluid. Nanofluid.*, 2014, **17**, 967.
24 J. Guzowski and P. Garstecki, *Phys. Rev. Lett.*, 2015, **114**, 188302.
25 J. Guzowski, P. M. Korczyk, S. Jakiela and P. Garstecki, *Soft Matter*, 2012, **8**, 7269.
26 M. J. Neeson, R. F. Tabor, F. Grieser, R. R. Dagastine and D. Y. C. Chan, *Soft Matter*, 2012, **8**, 11042.